

Manuscript Details

Manuscript number	PNFA_2018_36
Title	1 × 4 MMI Visible Light Wavelength Demultiplexer Based on GaN Slot Waveguide Structures
Article type	Full Length Article

Abstract

High transmission losses are the key problem that limits the performances of visible light communication (VLC) system that work on wavelength division multiplexing (WDM) technology. In order to overcome this problem, we propose a novel design for a 1×4 optical demultiplexer based on the multimode interference (MMI) in slot-waveguide structures that operates at 547 nm, 559 nm, 566 nm and 584 nm. Gallium-nitride (GaN) and silicon-oxide (SiO₂) were found to be excellent materials for the slot waveguide structures. Simulation results show that the proposed device can transmit 4-channels that work in the visible light range with a low transmission loss of 0.983-1.423 dB, crosstalk of 13.8-18.3 dB and bandwidth of 1.8-3.2 nm. Thus, this device can be very useful in visible light networking system that works on WDM technology.

Keywords	FV-BPM; MMI; WDM; Slot-Waveguide.
Corresponding Author	Dror Malka
Corresponding Author's Institution	Holon Institute of Technology (HIT)
Order of Authors	Dror Malka, TamirShoresh Shoresh, Nadav Katanov

Submission Files Included in this PDF

File Name [File Type]

Highlights good.docx [Highlights]

main paper1.pdf [Manuscript File]

To view all the submission files, including those not included in the PDF, click on the manuscript title on your EVISE Homepage, then click 'Download zip file'.

Highlights

- **Modeling a 1×4 wavelength demultiplexer based on the multimode interference (MMI) in a GaN slot-waveguide structures.**
- **Gallium-nitride and silicon-oxide were found to be excellent materials for the slot waveguide structures.**
- **The device can transmit 4-channels that work in the visible light range with a low transmission loss of 0.983-1.423 dB.**
- **The device can be useful in visible light networking system that work on WDM technology.**

1 × 4 MMI Visible Light Wavelength Demultiplexer Based on GaN Slot Waveguide Structures

Tamir Shores, Nadav Katanov and Dror Malka*

Faculty of Engineering, Holon Institute of Technology (HIT), Holon 5810201, Israel

* Correspondence: drorm@hit.ac.il

Abstract — High transmission losses are the key problem that limits the performances of visible light communication (VLC) system that work on wavelength division multiplexing (WDM) technology. In order to overcome this problem, we propose a novel design for a 1×4 optical demultiplexer based on the multimode interference (MMI) in slot-waveguide structures that operates at 547 nm, 559 nm, 566 nm and 584 nm. Gallium-nitride (GaN) and silicon-oxide (SiO₂) were found to be excellent materials for the slot waveguide structures. Simulation results show that the proposed device can transmit 4-channels that work in the visible light range with a low transmission loss of 0.983-1.423 dB, crosstalk of 13.8-18.3 dB and bandwidth of 1.8-3.2 nm. Thus, this device can be very useful in visible light networking system that works on WDM technology.

Index Terms— FV-BPM; MMI; WDM; Slot-Waveguide.

1. INTRODUCTION

The growing vast of developments in the visible light communication (VLC) systems requires [1-3] new and powerful waveguide components that can support high speed light communication with low transmission losses.

demultiplexers are an important part of optical communication networks and can be implemented using several techniques: multimode interference (MMI) couplers [4,5], Y-branch devices [6] and Mach-Zehnder interferometers [7].

A slot waveguide is a structure proposed of a narrow low index region surrounded by two layers of high index material [8]. This structure allows light to be strongly confined and guided through it [9] due to the total internal reflection effect [10].

MMI devices are commonly implemented in photonic integrated circuits due to their low losses, large optical bandwidth, and simple structure [11-15]. Self-imaging is an effect that occurs in waveguides based on MMI, by which the electric field profile that enters the device is duplicated into one or more images (depending on the geometry of the MMI) along the propagation axis of the device at periodic intervals [15].

GaN is a promising material for high-power and high temperature electronics due to its wide energy band gap and large critical electric field [16]. Recently, researchers assessed the performance of GaN based slot-waveguide device and found it suitable for transmitting visible light with 0.1–0.4 (dB/cm) transmission loss [17].

Moreover, researchers show the great potential of using a silicon (Si) slot-waveguide based MMI structures for designing splitters [18,19,20] and wavelength demultiplexers in the C-band range [12,21]. However, Si slot-waveguide is not suitable to use for transmitting light in the visible range due that Si has a high absorption losses. In order to overcome this problem, we propose to use GaN-SiO₂ slot-waveguide which enables to transmit visible light without confinement losses.

In this paper, a design of a 1×4 wavelength demultiplexer based on a multimode interference in a GaN–SiO₂ slot waveguide structure, that divides four channels in the visible light range, is presented. The selected wavelengths were found to be 547 nm (λ_1), 559 nm (λ_2), 566 nm (λ_3), 584 nm (λ_4).

The device is based on cascade of three 1×2 MMI couplers, six S-bands, six output tapers and one waveguide segment. The geometrical parameters of the MMI couplers and the slot-waveguide structure were analyzed in order to obtain strong field confinement and to find the optimal lengths of the MMI couplers. The simulations were carried out using the full vectorial-beam propagation method (FV-BPM) combined with Matlab codes.

2. THE 1×4 DEMULTIPLEXER STRUCTURE AND THEORETICAL ASPECT

Figure 1(a) shows the x-y cross sectional view at $z=0$ where the orange areas represent GaN, green and white areas represent SiO₂. H_{slot} is the height of the SiO₂ layer (slot area) and the height of the GaN layer, which is the slab area, is H_{slab} . n_{slot} , n_{slab} and n_{clad} are the refractive indexes of the slot, slab and cladding, respectively. Table 1 shows the refractive index values of n_{slot} , n_{slab} and n_{clad} at the operated wavelengths.

Table 1. The GaN and SiO₂ materials refractive index values for the operated wavelengths.

$\lambda(\text{nm})$	547	559	566	584
$n_{\text{slot}}=n_{\text{clad}}$	1.4792	1.4787	1.4784	1.4777
n_{slab}	2.416	2.4105	2.4075	2.4004

Figure 1(b) shows the x-z cross sectional view at $y=0$, where the three MMI couplers designed for the device are presented. The lengths of the MMI couplers are L_{MMI1} , L_{MMI2} , and L_{MMI3} , respectively and their width is W_{MMI} .

The width size of the input waveguide segment was chosen to be $0.3 \mu\text{m}$ with a height of $20 \mu\text{m}$. The width of the tapers varies from $0.34 \mu\text{m}$ to $0.3 \mu\text{m}$ (input/output) with a height of $5 \mu\text{m}$. The width size of S-Bands were chosen to be $0.3 \mu\text{m}$, to match the width size of the output taper, with a height of $40 \mu\text{m}$, and the distance between each one of them was chosen to be $0.1 \mu\text{m}$.

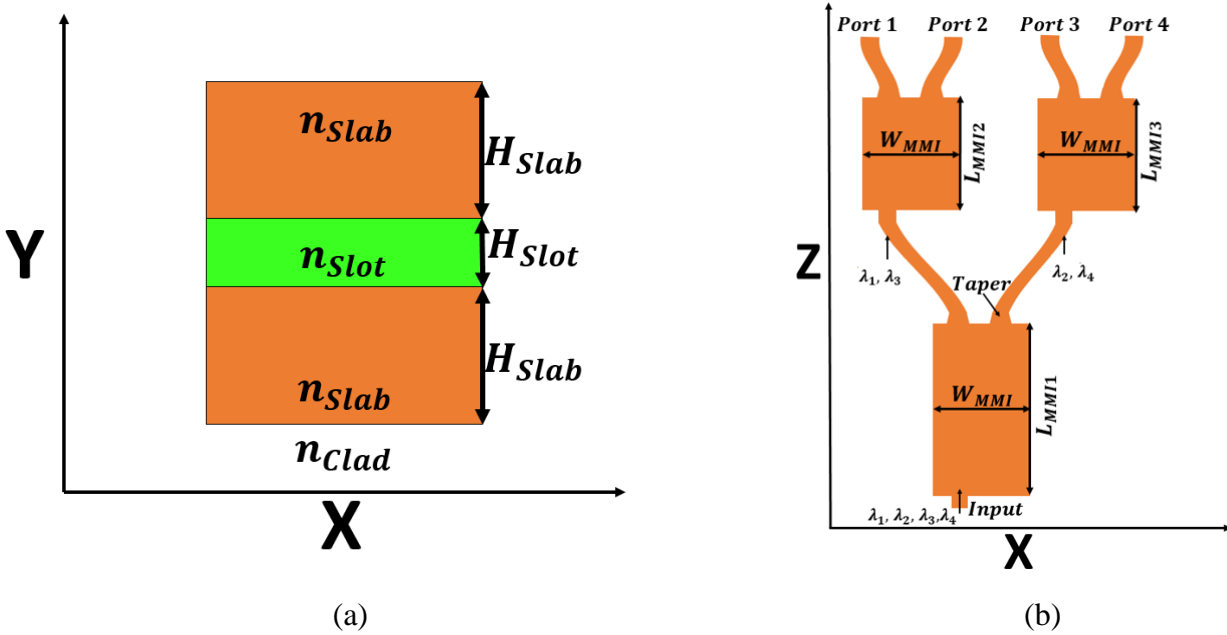


Fig. 1. An illustration of the 1×4 wavelength demultiplexer (a) in the x-y plane (b) in the x-z plane.

The MMI is based on the self-imaging effect, which means that every wavelength that enters the coupler will have a direct image of itself periodically. The distance from the point of entry to the point of the first image is called the beat length and it is given by [20]

$$L_{\pi}^n \approx \frac{4n_{eff} W_e^2}{3\lambda_n}; n=1,2,3,4. \quad (1)$$

Where n_{eff} is the effective refractive index of the fundamental mode in the core area, which include the slot and slab areas. The FV-BPM mode solver calculates this parameter. λ_n are the wavelengths that operate the device, and W_e is the effective width of the MMI couplers. The W_e size at the case of transverse electric (TE) mode is given by [20]:

$$W_e = W_m + \frac{\lambda_n}{\pi} (n_{eff}^2 - n_{Clad}^2)^{-1/2} \quad (2)$$

Where W_m is the width of the MMI coupler as seen in figure 1b.

In order to divide two different wavelengths using the MMI coupler, these conditions must be met:

$$\begin{aligned} L_{MMI2} &= p_1 L_{\pi}^{\lambda_1} = (p_1 + q_1) L_{\pi}^{\lambda_3} \\ L_{MMI3} &= p_2 L_{\pi}^{\lambda_2} = (p_2 + q_2) L_{\pi}^{\lambda_4} \end{aligned} \quad (3)$$

Where p is the integer, L_{π} is the beat length and q is an odd number.

In order to divide four different wavelengths into two outputs using the MMI coupler, this condition must be met:

$$L_{MMI1} = p_3 L_{\pi}^{\lambda_1} = (p_3 + q_3) L_{\pi}^{\lambda_2} = (p_3 + q_3 + 1) L_{\pi}^{\lambda_3} = (p_3 + q_3 + 2) L_{\pi}^{\lambda_4} \quad (4)$$

In order to cancel the third mode from inside the MMI, the input taper has been shifted $\pm(1/6)W_e$ from the center of the MMI. In addition, the lengths of the MMI couplers have been optimized to obtain better performances.

The insertion losses of the device are given by:

$$Loss(dB) = -10 \log \left(\frac{P_{out}}{P_{in}} \right) \quad (5)$$

Where P_{out} is the output power and P_{in} is the input power.

The crosstalk of the device is given by:

$$CT_n = \frac{1}{3} \sum_{m=1}^4 10 \log \left(\frac{P_m}{P_n} \right) \quad (6)$$

Where P_n is the power in the desirable port and P_m is the interfering power in the other port.

3. RESULTS

The Rsoft photonic CAD suite was used to simulate the device, and the optimization of it was calculated through FV-BPM simulations alongside Matlab codes. From these calculations, the optimal dimensions of the slot-waveguide were found to be: $H_{slot}=30$ nm, $H_{slab}=120$ nm, $W_{MMI}=1.2$ μ m.

Figure 2 shows the optimal size of the slot layer and the tolerance values (28.05-31.64 nm) around H_{slot} at 70-100% of the normalized intensity.

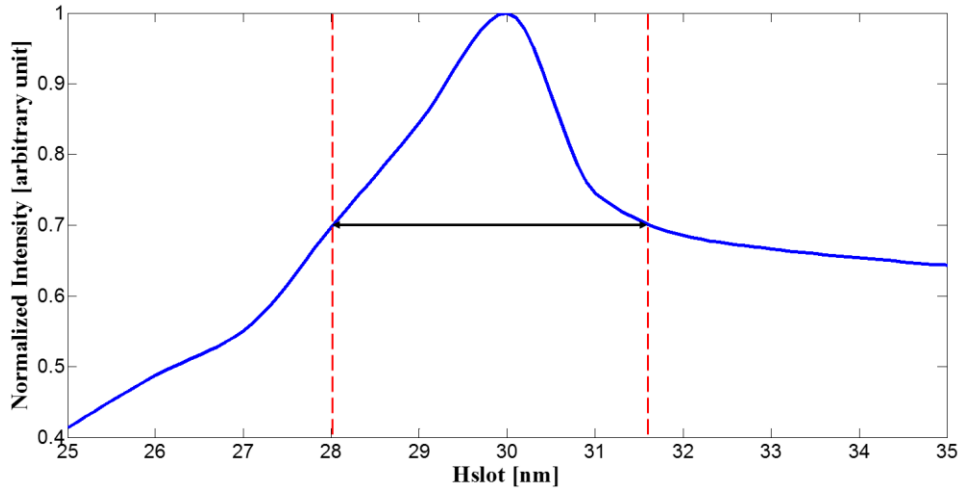


Fig. 2. Normalized Intensity as function of H_{slot} .

Figure 3(a) and (b) show the electric field patterns of the quasi-TE fundamental mode and minor mode in the x-y plane, for a wavelength of 559 nm. The strong confinement of light (red color) can be noticed in figure 3(a). The same profile field mode is obtained for the other operated wavelengths.

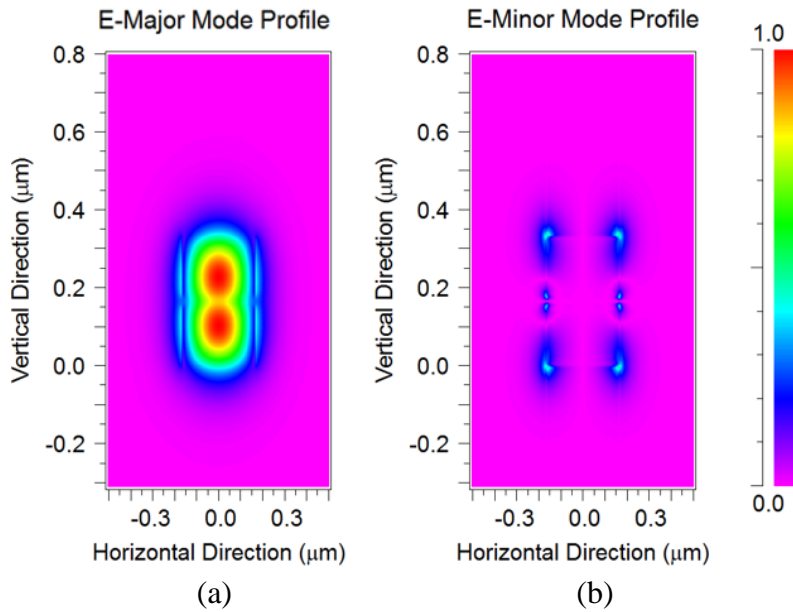


Fig. 3. Electric field patterns for quasi-TE fundamental mode for (a) E_x , (b) E_y .

The effective refractive indexes (n_{eff}) values were found by solving the major field mode for the operated wavelengths. Figure 4(a) show the n_{eff} as a function of the operated wavelengths.

Using n_{eff} and W_{MMI} values, equations (1) and (2) can be solved, and the effective width of the MMI (W_e) can be found along with the beat lengths of the operating wavelengths. Figure 4(b) presents the beat lengths as a function of wavelength.

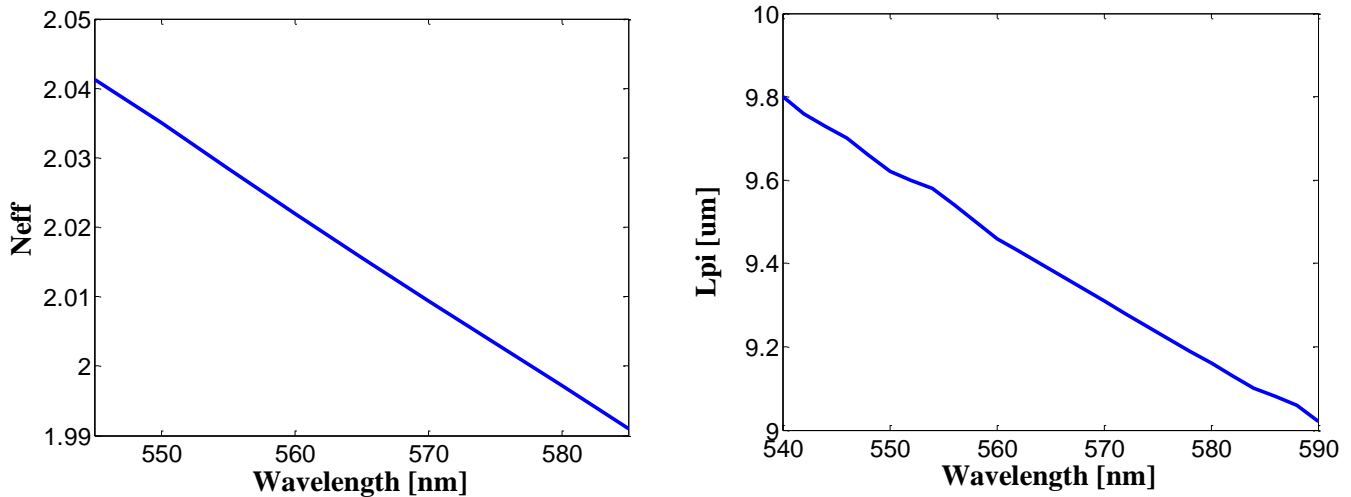


Fig. 4. n_{eff} and L_{π} function of the wavelength: (a). n_{eff} . (b). L_{π} .

Using the solutions of equations (3) and (4) that are presented in figure 5, alongside optimizations from the FV-BPM solver, the suitable lengths of each one of the three MMI couplers were found to be: $L_{\text{MMI1}}=453.2 \mu\text{m}$, $L_{\text{MMI2}}=157.5 \mu\text{m}$, $L_{\text{MMI3}}=158.1 \mu\text{m}$. As seen from the two blue arrows marked in figure 5, MMI1 is suitable for two wavelength pairs, which are 547 nm (λ_1) with 559 nm (λ_2) and 566 nm (λ_3) with 584 nm (λ_4). This means that 547 nm and 566 nm are propagated into MMI2 and 559 nm and 584 nm are propagated into MMI3. In a similar manner, the pink arrow points to the suitable length of MMI2, which divided 547 nm and 566 nm, and the green arrow points to the suitable length of MMI3, which divided 559 nm and 584 nm.

The wavelength pairs in figure 5 are: 547 nm with 550-590 nm (blue circles); 559 nm with 561-590 nm (green squares); 566 nm with 570-590 nm (red triangles); 584 nm with 587-590 nm (purple diamonds). It can be determined from this figure that the most suitable selected wavelengths for our proposed device are 547 nm, 559 nm, 566 nm and 584 nm.

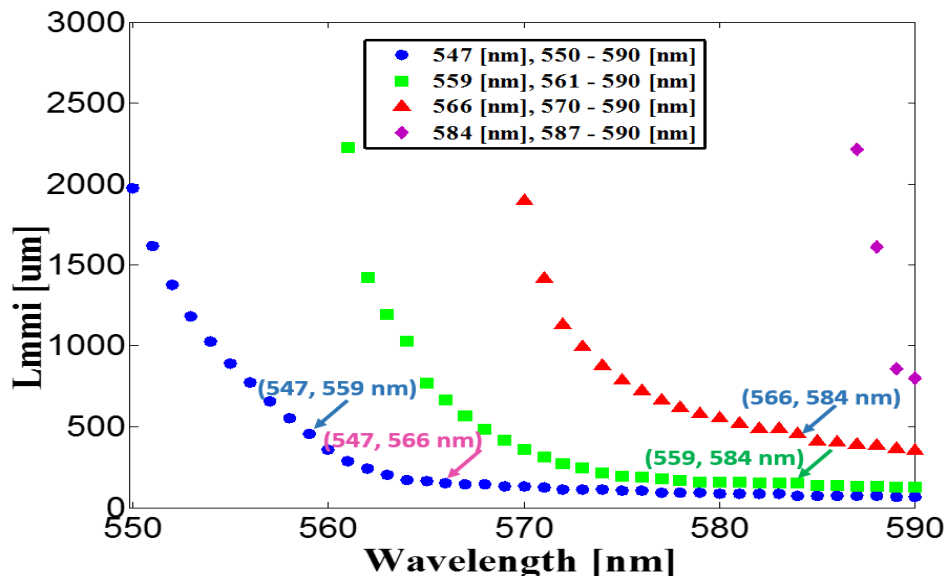


Fig. 5. MMI coupler lengths as a function of wavelength couples in a range of 547-590 nm.

Figures 6(a)-(d) show the field profile in the device for the operating wavelengths at x-z plane. From this figures, it can be noticed that the divided of the four operated wavelengths obtained at $z=475 \mu\text{m}$ (MMI1 coupler output). MMI2 coupler divided between $\lambda_1=547 \text{ nm}$ (port 2) and $\lambda_3=566 \text{ nm}$ (port 1) at $z=680 \mu\text{m}$ as shown in figures. 6(a) and (c). MMI3 coupler divided between $\lambda_2=559 \text{ nm}$ (port 4) and $\lambda_4=584 \text{ nm}$ (port 3) at $z=680 \mu\text{m}$ as shown in figures. 6(b) and (d).

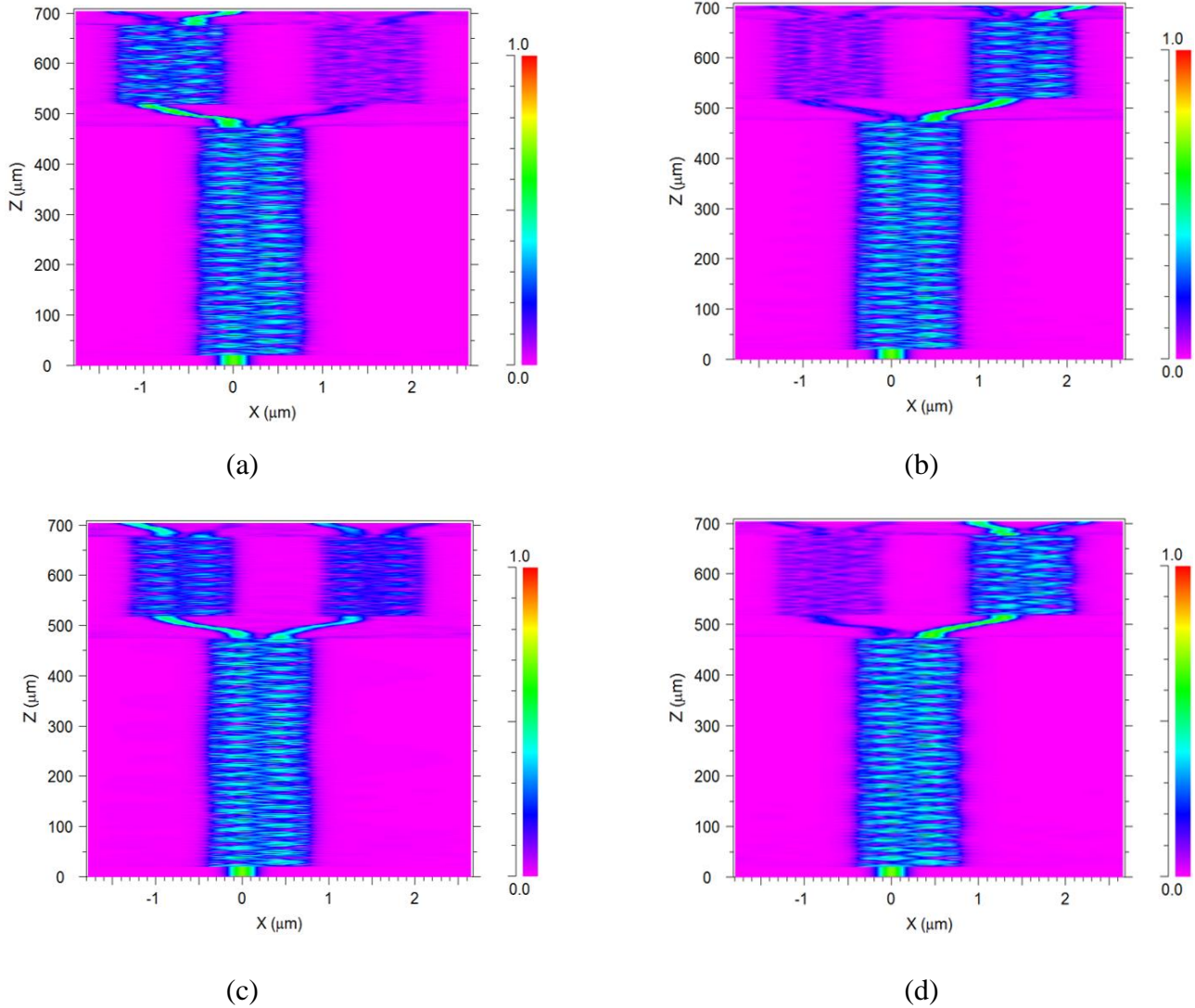


Fig. 6. Field distributions of the 1x4 MMI photonic wavelength demultiplexer (a) $\lambda_1=547 \text{ nm}$ (port 2); (b) $\lambda_2=559 \text{ nm}$ (port 4); (c) $\lambda_3=566 \text{ nm}$ (port 1); (d) $\lambda_4=584 \text{ nm}$ (port 3).

Figure 7 shows the spectral transmission of the four channels in the visible light range (545-585 nm). The crosstalk, insertion losses and full width half-maximum (FWHM) were found using figure 7 and equations (5) and (6) as shown in Table.2.

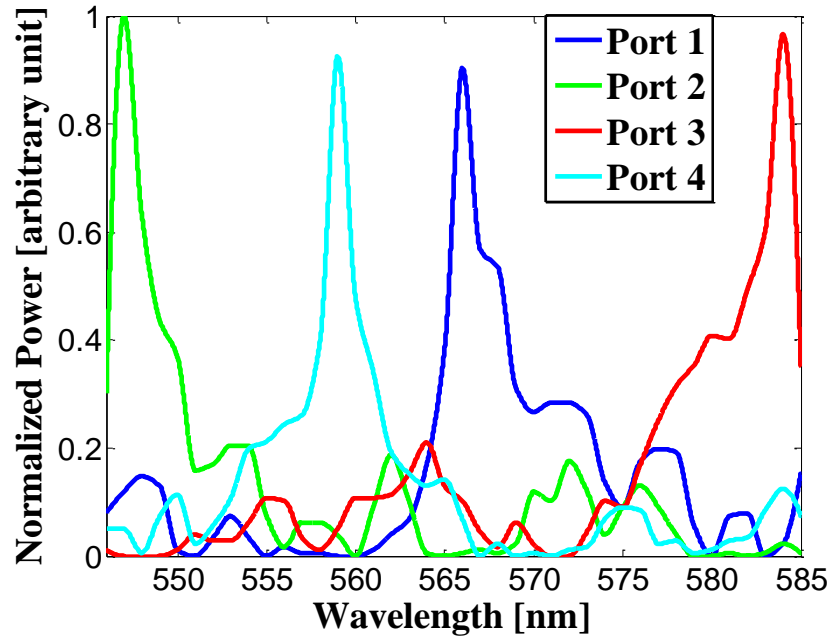


Fig. 7. Normalized power in each port as a function of wavelength.

Table 2: Crosstalk, Losses and FWHM values for the operating wavelengths.

$\lambda(\text{nm})$	547	559	566	584
Port	2	4	1	3
Crosstalk(dB)	17.059	18.316	14.423	13.82
Losses(dB)	0.983	1.315	1.423	1.133
FWHM(nm)	1.8	2.7	2.3	3.2

4. CONCLUSION

To conclude, this paper presents a design of a 1x4 MMI photonic wavelength demultiplexer based on a SiO₂-GaN slot-waveguide structure.

Results from the simulation software have shown the four operating wavelengths are 547 nm, 559 nm, 566 nm, 584 nm.

The propagation length of the whole device is 0.7 mm with crosstalk ranging between 13.82-18.316 dB, losses ranging between 0.983-1.423 dB and FWHM ranging between 1.8-3.2 nm. These values show that the suggested device can be useful, especially for optical networks that use WDM technology in the visible light range.

The functionality of the proposed device shows the great potential of using GaN slot-waveguide technology to increase performances in VLC system and the ability in future work to integrate on photonic chip.

ACKNOWLEDGMENTS

The authors gratefully acknowledge the financial support of the EU Horizon 2020 program towards the Internet of Radio -Light project H2020 -ICT761992.

REFERENCES

- [1] D. Tsonev, et al. "Towards a 100 Gb/s visible light wireless access network," *Optics Express*, vol. 23, pp. 1627-1637, Jan. 2015.
- [2] Y. Wang, et al. "4.5-Gb/s RGB-LED based WDM visible light communication system employing CAP modulation and RLS based adaptive equalization." *Optics express*, vol.23, pp. 13626-13633, May 2015.
- [3] G. Cossu, et al. "3.4 Gbit/s visible optical wireless transmission based on RGB LED," *Optics express*, vol. 20.26, pp. B501-B506, Dec. 2012.
- [4] S. Wei, et al. "A novel wavelength multiplexer/demultiplexer based on side-port multimode interference coupler." *International Society for Optics and Photonics*, vol. 9133, p.91330Y, May 2014.
- [5] B. Li, et al. "Low-loss $1/\sqrt{2}$ multimode interference wavelength demultiplexer in silicon-germanium alloy," *IEEE Photonics Technology Letters*, vol. 11, pp. 575-577, May 1999.
- [6] N. Goto, and G.L. Yip, "Y-branch wavelength multi/demultiplexer for $\gamma = 1.30$ and $1.55 \mu\text{m}$," *Electronics Letters*, vol. 26, pp. 102-103, Jan. 1990.
- [7] A. Tervonen, et al. "A guided-wave Mach-Zehnder interferometer structure for wavelength multiplexing," *IEEE photonics technology letters*, vol. 3, pp. 516-518, June 1991.
- [8] O. Katz, and D. Malka. "Design of novel SOI 1×4 optical power splitter using seven horizontally slotted waveguides," *Photonics and Nanostructures-Fundamentals and Applications*, vol. 25, pp. 9-13, July 2017.
- [9] R. Almeida, et al. " Guiding and confining light in void nanostructure," *Optics letters*, vol. 29, pp. 1209-1211, 2004.
- [10] KP. Bohannon, et al. "Refractive Index Imaging of Cells with Variable-Angle Near-Total Internal Reflection (TIR) Microscopy," *Microscopy and Microanalysis*, vol. 23, pp. 978-988, Sep. 2017.
- [11] JM. Heaton, and RM. Jenkins. "General matrix theory of self-imaging in multimode interference (MMI) couplers," *IEEE Photonics Technology Letters*, vol. 11, pp. 212-214, Feb. 1999.
- [12] D. Malka, et al. "Design of a 1×4 silicon wavelength demultiplexer based on multimode interference in a slot waveguide structures.", *Electrical & Electronics Engineers in Israel (IEEEI), 2014 IEEE 28th Convention of. IEEE*, pp. 1-4, Dec. 2014.
- [13] J. Xiao et al. "Design of an ultracompact MMI wavelength demultiplexer in slot waveguide structures", *Optics Express*, vol.15, pp. 8300-8308, June 2007.
- [14] M. Blahut, and D. Kasprzak, "Multimode interference structures—properties and applications," *Optica Applicata*, vol.34, pp. 573-587, 2004.
- [15] LB. Soldano, and E.Pennings. "Optical multi-mode interference devices based on self-imaging: principles and applications," *Journal of lightwave technology*, vol. 13, pp. 615-627, Apr. 1995.
- [16] W. Huang, et al. "Comparison of MOS capacitors on n-and p-type GaN," *Journal of Electronic Materials*, vol.35, pp.726-732, 2006.
- [17] X. Xiao, et al. "Designing gallium nitride slot waveguide operating within visible band," *Optical and Quantum Electronics*, vol. 47, pp. 3705-3713, Aug. 2015.
- [18] D. Malka, et al. "A Photonic 1×4 Power Splitter Based on Multimode Interference in Silicon–Gallium-Nitride Slot Waveguide Structures," *Materials*, vol. 9, p. 516, June 2016.
- [19] A. Zanzi, et al. "Compact and low-loss asymmetrical multimode interference splitter for power monitoring applications," *Optics letters* vol. 41, pp. 227-229, Jan. 2016.
- [20] D. Malka, et al. "Slot silicon-gallium nitride waveguide realizing 1×4 optical power splitter," *Science of Electrical Engineering (ICSEE), IEEE International Conference on the. IEEE*, pp. 1-5, Nov. 2016.
- [21] BB. Ben Zaken, et al. "An 8-channel wavelength MMI demultiplexer in slot waveguide structures." *Materials*, vol. 9, p.881, 2016.